J. Adhesion Sci. Technol., Vol. 21, No. 7, pp. 559–574 (2007)

Also available online - www.brill.nl/jast

Adhesive properties of a radial acrylic block co-polymer with a rosin ester resin

F. SIMAL [1,*], M. JEUSETTE [2], PH. LECLÈRE [2], R. LAZZARONI [2] and P. ROOSE [1]

[1] *Research & Development, Cytec Surface Specialties S.A., Anderlechtstraat 33, B-1620 Drogenbos, Belgium*
[2] *Service de Chimie des Matériaux Nouveaux, Université de Mons-Hainaut, Place du Parc 20, B-7000 Mons, Belgium*

Received in final form 5 February 2007

Abstract—A novel four-arm radial block co-polymer $(A\text{-}B)_4$ obtained by atom transfer radical polymerization (ATRP) and a random (statistical) co-polymer of similar composition have been prepared. In the presence of rosin esters, these materials show pressure-sensitive adhesive (PSA) properties. The aim of this investigation was to study the relationship between the molecular architecture of tackified systems and their typical PSA properties. First, the miscibility of these two co-polymers with a rosin ester resin was investigated. Then, the performance of PSA such as peel strength and shear resistance was studied. In contrast to the random co-polymer, the block co-polymer presents two glass transitions, as evidenced by DSC and TMA. Atomic force microscopy (AFM) further confirmed the well-defined microphase separation. The Gordon–Taylor expression provides an empirical description of the dependence of the T_g on the tackifier content for the random co-polymer and the elastomer phase of the block co-polymer. The DSC results also suggest that the thermoplastic microdomains are partly miscible with the tackifier. In terms of PSA properties, it was observed that the peel strength was improved as the amount of tackifer in the blend was increased. Although the addition of rosin ester led to a significant drop of the cohesive strength of the random co-polymer, the network present in the block co-polymer made it possible to reach the required cohesion for suitable adhesive performance in PSAs.

Keywords: Radial block co-polymer; ATRP; pressure-sensitive adhesives; tackifier.

1. INTRODUCTION

Since the mid-1960s, thermoplastic elastomers based on styrenic block co-polymers (SBCs) have found a wide use in the field of pressure-sensitive adhesives (PSAs) [1].

*To whom correspondence should be addressed. Tel.: (32-2) 334-5761; Fax: (32-2) 378-3944; e-mail: francois.simal@cytec.com

The success of these materials over the years can certainly be related to their microphase structure which is due to the immiscibility between the soft and hard polymer segments [2]. The polystyrene domains, which act as thermally reversible physical cross-links, make these materials thermo-processable. Thus, solvent-free systems can be applied as hot-melts which provide an environmentally-friendly solution for adhesive coaters.

However, SBCs do not possess any PSA properties as such. In order to achieve sufficient tack, these co-polymers need to be compounded with the proper types and levels of additives, typically tackifying resins and processing oils which tend to mix selectively in either hard or soft phase. This particular feature offers a significant formulation window and provides a very broad range of adhesive performance. The effect of tackifying resins on the adhesive properties of SBCs has been studied extensively. A considerable amount of research has been devoted to the correlation of the linear visco-elastic properties obtained by dynamic mechanical analysis (DMA) with the usual PSA parameters such as tack, peel strength and shear strength [3–6].

Although a great deal of effort had been spent in the past for the improvement of specific properties and coating conditions of SBCs, extensive research was pursued later to improve tack, adhesion on polar substrates, shear adhesion failure temperature (SAFT), ageing and UV-resistance, solvent resistance and processability, such as the hot-melt stability and the label conversion. Ageing, UV-resistance and melt viscosity could be improved by the introduction of hydrogenated SBCs. Also, the addition of di-blocks and, more recently, polyisoprene to SBCs led to enhanced tack and wetting properties [7–10]. Modifications of the topology of the polymer architecture through variations in the polymer synthesis resulted in the development of block co-polymers with radial architectures showing higher cohesion and a desirable hot-melt viscosity [11]. Finally, very recent developments have led also to the design of new compositions such as polystyrene-block-polyisoprene/butadiene-block-polystyrene with higher tack, controlled hot-melt viscosity and better compatibility with hydrocarbon resins [12].

Despite these benefits, the development of all-acrylic counterparts of SBCs has always been a long-sought goal. Due to the inherent and adjustable adhesion power of acrylates, acrylate block co-polymer systems are expected to perform better in terms of durability, resistance to photodegradation, heat resistance, tack and moisture vapour transmission rate as compared to SBCs. Moreover, the addition of a tackifier is usually not a prerequisite for acrylate-based systems.

In the last decade, major advances to gain control over radical polymerization have been realized. Among these new polymerization techniques, the atom transfer radical polymerization (ATRP) stands out as a very efficient and practical method to prepare (meth)acrylic block co-polymers of different architectures. Many examples of polymethacrylate-block-polyacrylate-block-polymethacrylate co-polymers prepared by controlled radical polymerization can be found in the literature [13]. Some work on the use of acrylic block co-polymers formulated as PSAs has been

published. These reports essentially deal with linear triblock co-polymers based on poly(n-butyl acrylate) (as the central segment) prepared either by atom transfer radical polymerization or by living anionic polymerization [14–16].

Meanwhile, star/radial (co)polymers have gained increasing interest in research and industry due to their unique structure and properties as compared to their linear counterparts [17–19]. At Cytec, we focussed on the development of "all acrylic" block co-polymers with radial architectures, based on poly(2-ethylhexyl acrylate-co-methyl acrylate) and poly(methyl methacrylate) and synthesized by means of ATRP. The synthesis, the molecular characteristics as well as the supramolecular structure (e.g., microphase separation) of these block co-polymers will be presented elsewhere [20]. The aim here is to show that industrially relevant PSAs can be obtained from radial acrylate block co-polymers. We report more specifically on the properties of adhesive compositions based on a radial block co-polymer and a hydrogenated rosin ester tackifier. The results are discussed with respect to a resin/polymer system based on a random co-polymer of similar composition showing no inherent microphase separation.

As an essential property of polymeric materials, the glass transition characteristics of the adhesives are reported systematically. The phase behaviour of the polymer/resin blends is discussed from these data.

The adhesive properties were determined according to standard methods, where tack, cohesion and peel strength form the basic set of data required for commercial purposes. As shown by several authors, however, carefully controlled and elaborate experiments should be conducted in order to unravel the interfacial and dissipative mechanisms involved in the overall adhesion behavior. As a few examples, we cite the experimental approach used by Creton and Fabre [21], where probe tack measurements coupled with optical imaging are explained in terms of linear and non-linear viscoelasticity, the work of Marin and co-workers [22] which emphasizes the relation between peel strength and viscoelasticity, and the work of Benyahia and co-workers [23, 24], where the peel properties (strength, behaviour and failure mechanisms visualized by a video system) were related to viscoelasticity, elongational viscosity and surface energetics. In most of the studies on adhesion mechanisms, the characteristic deformation rate of the materials and the temperature are used as primary experimental variables. Being aware of the limitations, we have merely attempted to relate the adhesion data to the small-strain (linear) viscoelastic properties of the adhesives. This simple approach often provides helpful indications to a first approximation.

2. EXPERIMENTAL

2.1. Polymer, tackifier and adhesive characteristics

A four-branched radial block co-polymer (B) was prepared by ATRP in a one-pot two-step synthesis. The structure of the block co-polymer is depicted schematically

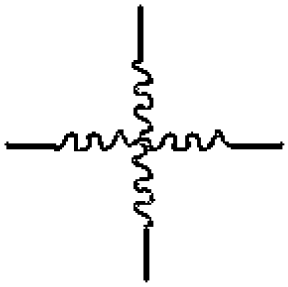

Figure 1. Schematic representation of the radial block co-polymer B. The curved and straight lines stand for P(2-EHA-co-MA) and PMMA segments, respectively.

in Fig. 1. The core segments, prepared in the first step of the synthesis, were composed of poly(2-ethylhexyl acrylate-co-methyl acrylate) and formed the soft elastomeric part of the polymer. The outer thermoplastic segments were essentially based on methyl methacrylate (MMA). However, about 10% of 2-ethylhexyl acrylate (2-EHA) and methyl acrylate (MA), remaining unreacted at the end of the first synthesis step, were also incorporated into the outer segments. The relative 2-EHA/MA/MMA monomer ratio in the block co-polymer was 58:25:17 wt%. By taking into account the monomer conversion at each reaction step (as determined by gas chromatography), the final weight ratio of MMA in the co-polymer was estimated to be 17%. The procedure to obtain the radial block co-polymer by means of ATRP is described in more detail elsewhere [20].

For comparison purpose, a statistical (random) branched co-polymer (S) of the same monomer composition as the block co-polymer was also prepared by conventional free radical polymerization initiated by 2,2′-azobisisobutyronitrile (AIBN) in ethyl acetate. Pentaerythritol tetrakis (3-mercaptopropionate) was used as the chain transfer agent in order to introduce branching in the polymer. Only less than 5% of free residual thiol groups were found after polymerization, which confirmed the efficiency of the chain transfer agent and thus the branched architecture of the statistical polymer.

The tackifier resin, Foral 85E, is a hydrogenated rosin ester and was used as supplied (Eastman).

The molecular weight distributions of the polymers and the tackifier were determined by size-exclusion chromatography with respect to a polystyrene standard. The number- and weight-average molecular weight values are reported in Table 1 and show that the S and B co-polymers are very similar in terms of molecular weight distribution ($M_w/M_n \approx 5$–6).

The adhesive materials were prepared by blending the acrylic polymers and the dissolved tackifier resin (50 wt% in ethyl acetate). The solutions were mixed for 24 h at room temperature.

The resin was added to the polymer in the amounts of 20, 33.3 and 42.8 wt% (or equivalently 25, 50 and 75 parts per hundred resin (phr)). The samples are

Table 1.
Molecular weight and glass-transition temperature of the polymers and the tackifier

	$M_{n,SEC}$	$M_{w,SEC}$	T_g (°C)
B-polymer	48.7	357	−40/50
S-polymer	49.4	327	−22
Foral 85E	0.46	0.55	36

denoted with a prefix S or B for the statistical (random) and the block co-polymers, respectively, followed by the amount of tackifier expressed in phr.

2.2. Thermal analysis

Uniform adhesive films were prepared by casting the adhesive solutions (≈30 wt% in toluene) in an aluminum cup covered with a silicone release paper. The solvent was evaporated for at least 72 h at room temperature. The film was subsequently dried at 110°C for approximately 2 h in order to remove residual solvent traces. The film thickness was typically in the range 0.3 to 0.5 mm.

The glass transition temperatures (T_g) were measured by differential scanning calorimetry (DSC) using a Q10 DSC equipment from TA Instruments. The DSC experiments were conducted dynamically at a heating rate of 20°C min^{-1}. The T_g values were determined at half heights of the transitions.

The softening temperatures (T_s) of the adhesives were determined from indentation profiles obtained by static thermo-mechanical analysis (TMA). The experiments were conducted with a 2940 TMA equipment from TA Instruments equipped with a flat-punched circular probe (diameter 2.58 mm). The heating rate was 10°C min^{-1}. The T_s values at the onset of penetration were determined from the gradients of the indentation profiles.

The shear storage and loss moduli were determined by dynamic mechanical analysis. A UDS200 rheometer from Paar-Physica in parallel plate geometry (diameter 25 mm) was used for the oscillation measurements. The angular frequency was varied from 0.1 to 100 s^{-1}. The strain deformation was fixed at 1% and the temperature was 23°C (Peltier heat regulator).

2.3. Adhesive properties

The adhesives were prepared by transfer coating. Here, a thin liquid film of the adhesive solution was applied on a silicone paper using an automatic bar coater. The drying conditions were as follows: 30 min at room temperature followed by 3 min at 110°C. The dried film (thickness ≈ 30 µm) was then laminated with a 23-µm-thick Mylar film. The laminate was conditioned for 24 h under controlled humidity and temperature (23 ± 2°C, 50 ± 5% RH) before testing.

Peel tests at a peel angle of 180° were performed according to FINAT FTM 1 specifications. PSA strips of 25 × 90 mm were applied on stainless steel (SS) plates

or high density polyethylene (HDPE) plates using a 2-kg FINAT standard test roller. The peel tests were conducted after dwell times of 20 min and 24 h with an Instron Tensile tester model 5543 at a peel rate of 300 mm min^{-1}. The static shear tests were performed according to FINAT FTM 8 specifications, utilizing a 25 × 25 mm or 12.5 × 12.5 mm contact area and a load of 1 kg.

2.4. Atomic force microscopy (AFM)

2.4.1. Film preparation. Thin films of the co-polymers were prepared by solvent casting from 20 ml toluene solution (10 mg ml^{-1}) on freshly-cleaved mica substrates. The samples were first analyzed after a complete evaporation of the solvent at room temperature for 48 h and then heated to 140°C, i.e., above the glass transition temperature of the thermoplastic segments (PMMA), under high vacuum (10^{-7} Torr) for 24 h.

AFM images were recorded in the tapping mode (TMAFM) using a Nanoscope IIIa microscope operated at room temperature in air. Commercial silicon cantilevers with a spring constant of 30 N m^{-1} were used.

3. RESULTS AND DISCUSSION

3.1. Glass transition and miscibility

The glass transition temperature (T_g) of an amorphous blend provides indication about the extent of miscibility between the components, at least at the molecular level. Hence, thermal analysis, and especially DSC, is well-suited for the study of the phase behaviour of a polymer and a tackifying resin. Figure 2a shows the DSC thermograms of the statistical and the block co-polymers. For the random (statistical) co-polymer (upper trace), a single glass transition is observed at a temperature of −22°C, which is in good agreement with the value predicted from the composition according to the Fox equation, i.e., −24°C. For the investigated random co-polymer/tackifier blend range, a single glass transition was always observed and this provides evidence of a homogeneous phase (the films were also optically clear). The action of a tackifier is generally termed as "anti-plasticizing" in the sense that the polymer matrix is diluted with a high-T_g compound, concomitantly increasing the T_g of the blend and reducing the Young's modulus in the rubbery state. In Fig. 3a, the T_g is shown as a function of tackifier content for the branched statistical co-polymer. The solid line results from a non-linear least-squares comparison of the data to the phenomenological Gordon–Taylor expression,

$$T_g = \frac{w_1 T_{g1} + k w_2 T_{g2}}{w_1 + k w_2}, \tag{1}$$

where w_1 and w_2 represent the mass fractions of the components and T_g, T_{g1} and T_{g2} are the T_g values of the blend and the two pure components, respectively. k is an

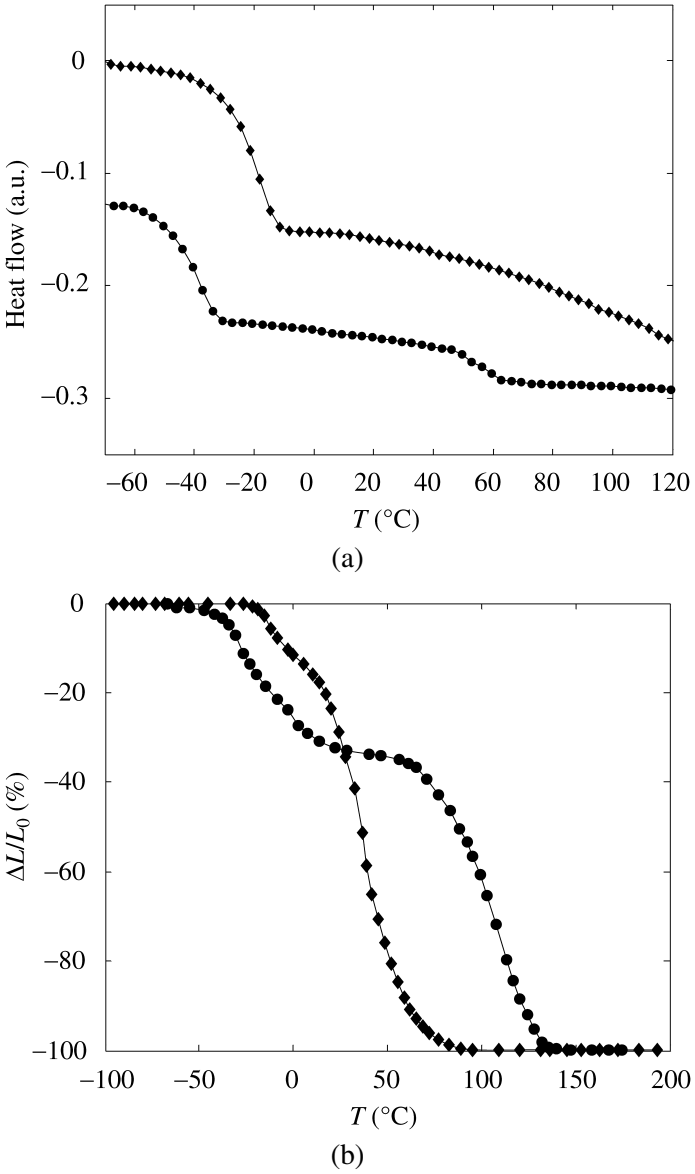

Figure 2. (a) DSC thermograms and (b) TMA profiles of the branched statistical co-polymer, S, (diamonds) and radial block co-polymer B (circles). The vertical axis represents the probe displacement ($\Delta L = L - L_0$), relative to the initial sample thickness, L_0.

empirical parameter. After fitting equation (1) to the data, a value $k = 0.53 \pm 0.04$ is reported for the Foral 85E/S blends. The T_g value of Foral 85E is 36°C.

Similar conclusions are obtained from the TMA data. In Fig. 2b, the indentation profile shows a marked penetration step (with an unexplained shoulder at the begin-

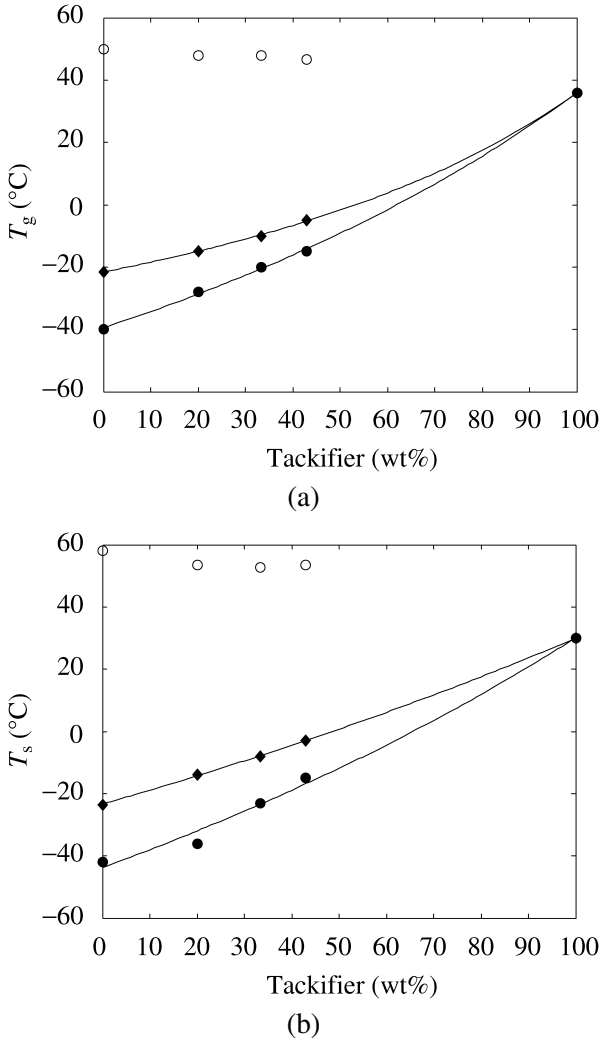

Figure 3. Plot of the glass-transition temperature T_g (a) and the softening point T_s (b) as a function of tackifier content. The diamonds show the data for the polymer/tackifier blends based on the random co-polymer S. For the block co-polymer/tackifier systems, the solid and the open circles refer to the transition of the elastomer matrix and the thermoplastic domains, respectively. The lines result from a non-linear least-squares comparison of the Gordon–Taylor equation (equation (1)), to the data.

ning) for the statistical co-polymer. Penetration starts at the softening temperature $T_s = -24°C$, in line with the T_g value. The dependence of T_s upon tackifier content in the blends is presented in Fig. 3b. Here, a value of $k = 0.83 \pm 0.04$ was found after least-squares regression of equation (1) to the data.

The observed phase homogeneity for the statistical co-polymer blended with Foral 85E is in good agreement with the studies of Kim and Mizumachi [25–27]

on the miscibility of acid-free acrylic co-polymer with modified rosins of limited bulkiness.

The lower DSC trace in Fig. 2a was obtained for the radial block co-polymer and exhibits two glass transitions typical for a phase-separated material.

The lower glass transition at −40°C is characteristic of the continuous soft matrix and agrees with the value predicted from the Fox equation. In contrast, the second glass transition occurs at a lower temperature ($T_g = 50$°C) than expected for pure PMMA segments. In our experimental conditions, a T_g of 120°C is measured for PMMA of high molecular mass. At a molecular mass of 10 kDa, the T_g decreases to 102°C due to end-group contributions. The presence of residual 2-EHA and MA at the end of the first step of the synthesis followed by co-polymerization with MMA during the second step presumably is responsible for the measured T_g of the outer blocks. An estimation of T_g based on the conversion of the residual amounts of 2-EHA and MA (as determined by gas chromatography) and the converted amount of MMA yields a $T_g = 57$°C according to the Fox expression. This is in fair agreement with the experimental value if one takes into account that end group effects are negligible.

Additional data were obtained using the tapping mode AFM which is an established technique for the characterization of the phase-morphology of block co-polymers [28–31]. The film surface characterized by the phase image in Fig. 4 clearly shows a regular assembly of bright dots on a dark background, which can be assigned to PMMA spheres embedded in a matrix of P(2-EHA-co-MA). The very low surface roughness measured from the height image (≈0.5 nm) further confirms that the phase contrast is essentially due to different elastic responses from the

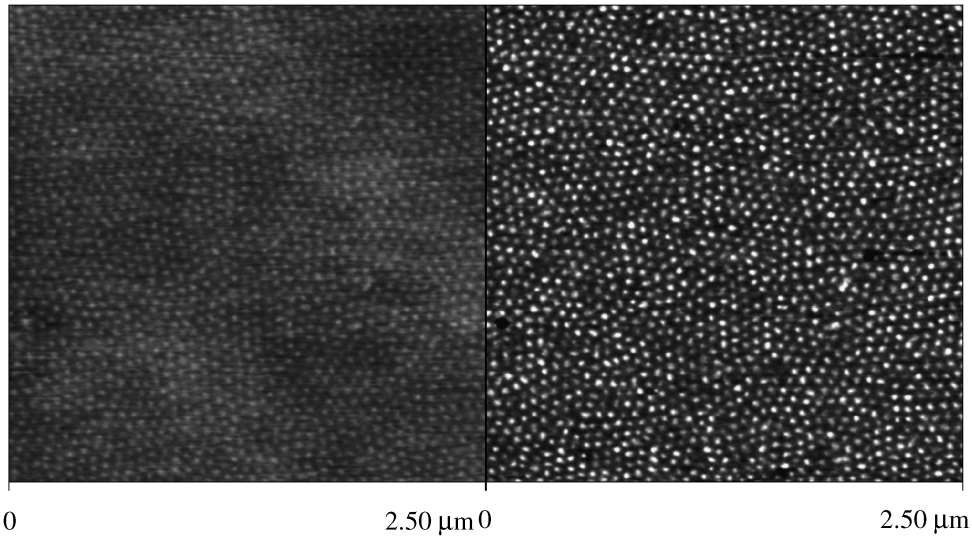

Figure 4. 2.5 × 2.5 µm^2 AFM height (left) and phase (right) images of the radial block co-polymer after annealing for 24 h at 140°C.

elastomeric and thermoplastic components of the block co-polymer. From a power spectrum analysis of the phase image, the size of the bright dots is estimated to be 30 ± 5 nm with an average centre-to-centre distance of 60 ± 5 nm.

A two-dimensional isotropic Fourier transform of the image further suggests that the domain periodicity is fairly sharp but reveals no further ordering at a larger length scale.

The actual PMMA content in the radial block co-polymer is ≈ 16 vol%, according to the segmental composition. For this composition range, the reported hexagonal pattern of PMMA spheres in a P(2EHA-co-MA) matrix is in agreement with previous data for similar thermoplastic elastomers [20].

As expected, thin films of the statistical co-polymer show no specific microstructure, consistent with the absence of phase separation.

The essentially biphasic nature of the block co-polymer was preserved upon blending with Foral 85E in the explored composition range. The T_g-values of the hard and soft blocks are plotted in Fig. 3a. In analogy to the statistical co-polymer, a non-linear increase of T_g is noted for the elastomeric part of the blend, which reflects the miscible character of the tackifier with the soft segments. A fit of equation (1) to the data yields a k value of 0.67 ± 0.08. The results are less conclusive for the hard domains where just a slight T_g decrease of a few degrees is noticed within the blend range. In this case, the T_g values of the outer segments and the tackifier are too close to evidence clearly any miscibility behaviour. However, partial miscibility of Foral 85E within the hard domains was also suggested from a similar experiment using a block co-polymer with outer segments of higher T_g ($\approx$80°C).

The TMA profile of the block co-polymer in Fig. 2b shows two distinct indentation steps separated by a rubbery plateau. The steps are assigned to the softening of the elastomeric matrix and the thermoplastic domains, respectively. In contrast to the DSC thermogram, the second transition is much more pronounced in the TMA curve. However, although the softening temperature at the first indentation step could be estimated easily, this was not always true for the second one at higher temperatures. Especially for the polymer/tackifier blends showing an overlap of the two indentation steps the onset of the second penetration could not be resolved clearly. Hence, the T_s values of the soft phase shown in Fig. 3b are more reliable than those of the hard phase. For the soft phase, an increase of T_s is again observed upon blending with Foral 85E. The estimated k value is 0.76 ± 0.33. From the previous considerations, we only note that the T_s values of the hard domains do not vary very much.

3.2. Adhesive properties

Although acrylic PSAs can be designed without the specific need for resin modifier for most applications, the use of a compatible tackifier is a recognized way to improve tack and peel strength, especially on low-surface-energy substrates such as polyethylene and polypropylene.

In this section, the influence of the level of Foral 85E on the peel strength of the adhesives based on the statistical and block co-polymers is discussed. At this stage, it is interesting to point out that the pure acrylic block co-polymer does not possess any PSA properties as such. It is only upon addition of a suitable tackifying resin that sufficient tack and peel strength were achieved.

The peel strengths measured after dwell times of 20 min and 24 h on stainless steel (SS, surface energy $\approx$ 40 mJ m^{-2}) and high density polyethylene (HDPE, surface energy $\approx$ 30–35 mJ m^{-2}) are reported in Figs 5 and 6.

As shown, an increase of the tackifier content enhances the peel strength on both relatively polar and non-polar substrates. Whereas the improvement in peel strength is only modest for the S-co-polymer, it increases by about a factor of two when the tackifier content is tripled (25–75 phr) in the B-co-polymer. The dwell time has no particular influence on the peel strength on stainless steel but results in a substantial improvement on HDPE for both polymers. The un-cross-linked statistical co-polymer exhibits significant peel strengths but the maximum is eventually achieved by the block co-polymer with 75 phr of Foral 85E for both substrates. Although rosin esters are known as good adhesion promoters for low-surface-energy substrates, the excellent balance of adhesion on both polar and non-polar substrates for the tackified block co-polymer definitely merits to be emphasized. These findings are consistent with the study of Takashima and Hata [32], which shows that the addition of a resin that is compatible with the rubber phase of a polymer increases the peel strength up to a maximum typically reached at 75 phr of resin.

In all the peel experiments, interfacial failure between the adhesive and the substrate was observed visually. This is the common failure mode at moderate and high peel rates (e.g., 300 mm min^{-1}) [23]. This type of failure has been addressed

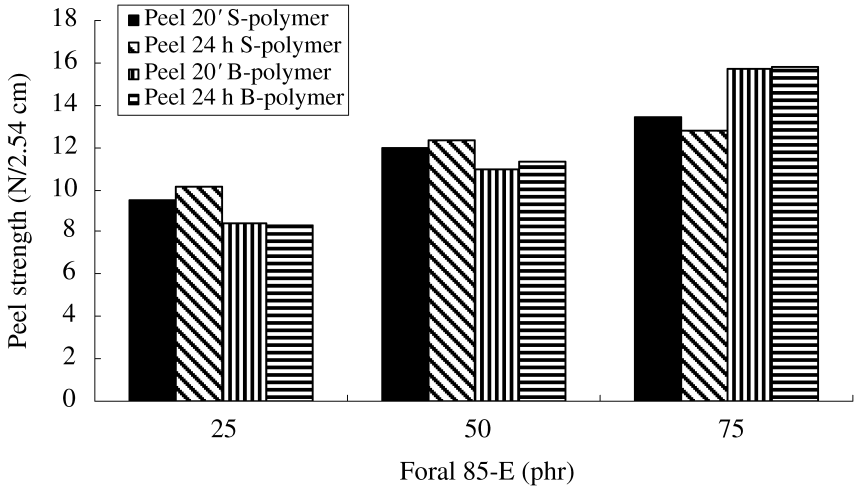

Figure 5. Peel strength (180°) on stainless steel after dwell times of 20 min and 24 h for the S and B co-polymers blended with Foral 85E tackifier at different levels.

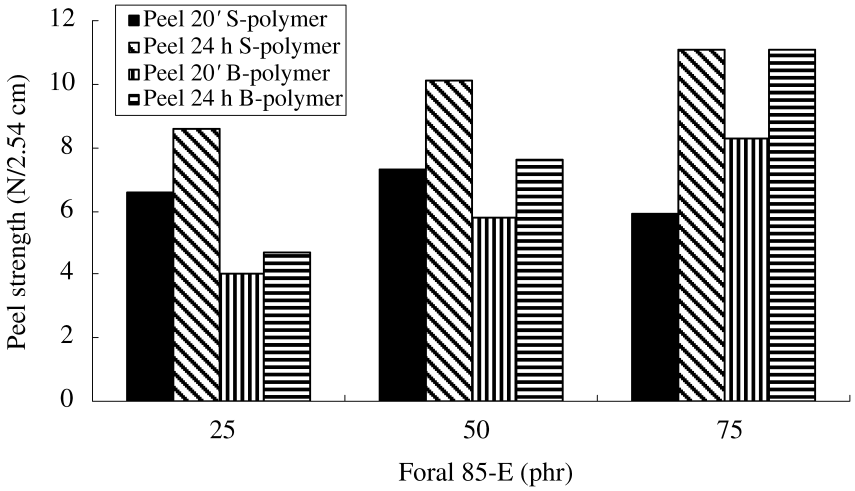

Figure 6. Peel strength (180°) on HDPE after dwell times of 20 min and 24 h for the S and B co-polymers blended with Foral 85E tackifier at different contents.

in a phenomenological way by several authors. It has been shown that the peel energy (P) required to detach the adhesive from the substrate is proportional to the thermodynamic work of adhesion w, i.e., $P = w\phi$, where ϕ stands for the energy dissipation factor and is related to the rheological characteristics of the adhesive [33, 34]. Given the complexity of debonding in a peel test (especially at 180°) and the limited data, we will not address the possible mechanisms in further detail here and we refer to other references dealing with the subject [22–24, 35].

Instead we will limit ourselves to a straightforward comparison of the peel behaviour with the small-strain visco-elastic characteristics of the adhesives under the assumption that the rheological properties govern the peel adhesion. Figure 7 shows the dependence of the storage (G') and the loss G'' moduli for the two co-polymers, S (Fig. 7a) and B (Fig. 7b), with 25 and 75 phr of tackifier. Within the experimental angular frequency range, both G' and G'' increase with tackifier content due to the shift of the glass transition towards lower frequencies.

From these data, the empirical criterion of Dahlquist [3], which prescribes the requirement for proper bond formation, can be verified. It states that the tensile elastic modulus E' ($\approx$3G′) should be lower than 0.1 MPa in a timescale of 1 s (i.e., $\omega_1 \approx 2\pi$ rad s^{-1}) typical for the bonding process. This criterion is closely met for the S-co-polymer but not fully for the B-co-polymer where E' exceeds the limit. From the correspondence between the peel rate and the angular frequency in dynamic mechanical analysis, a rough estimate of the characteristic debonding frequency in a peel test at 300 mm min^{-1} can be obtained i.e., $\omega_2 \approx$ 300 rad s^{-1}. Following the viscoelastic guideline stating that P is proportional to $G''(\omega_2)/G'(\omega_1)$ and by extrapolation of the G'' data in Fig. 7 to 300 rad s^{-1}, relative changes in peel strength can be predicted [36, 37]. For instance, for an increase from 25 to 75 phr of tackifier, increases of the peel strength by factors of

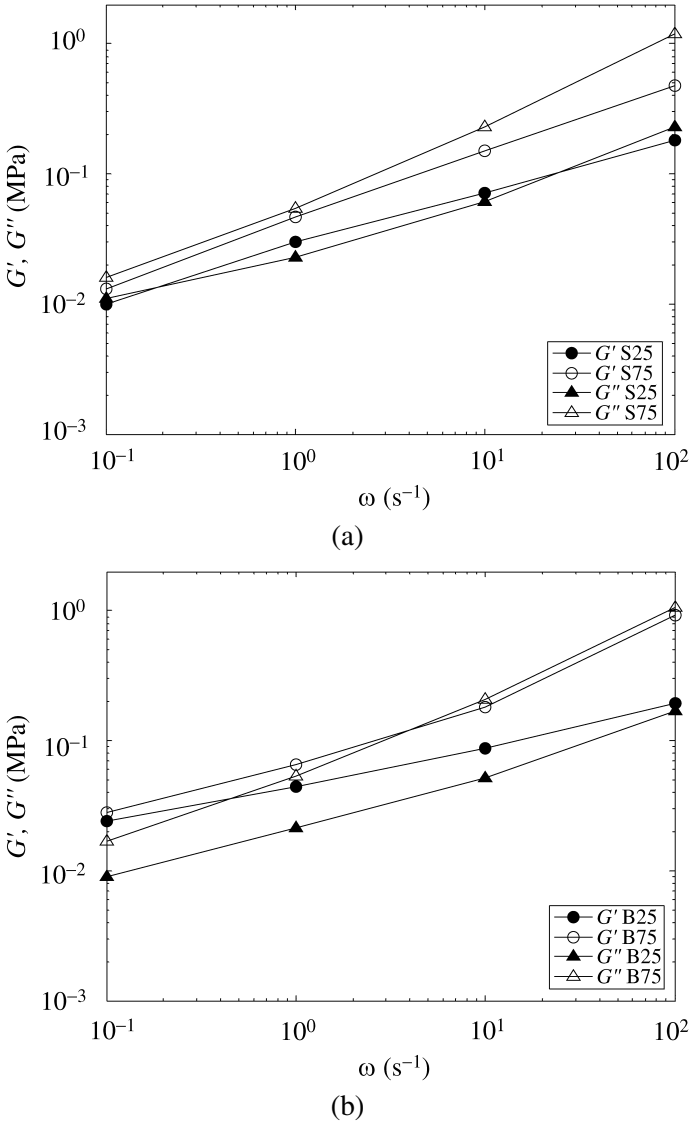

Figure 7. Small-strain viscoelastic moduli, G' and G'', in the angular frequency range [0.1, 100] rad s^{-1} for the S (a) and B (b) co-polymers with 25 and 75 phr of tackifier.

3 and 4 are calculated for the S- and B-co-polymers, respectively. Obviously, this overestimates the results shown in Figs 5 and 6, but still it suggests a stronger effect of the tackifier content for the block co-polymer, as observed.

Axisymmetric probe tack tests are more convenient to investigate adhesion mechanisms with regard to the molecular characteristics of the adhesive. Preliminary data show, however, that the radial block co-polymer without tackifier detaches from the

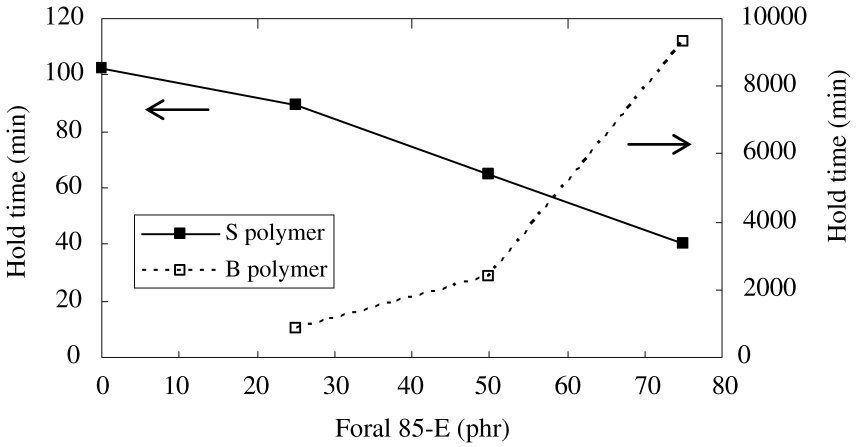

Figure 8. Hold time in a shear test *versus* Foral 85E content for the S- and B-co-polymer systems. Note that the initial load was increased by a factor of four in the case of the B-systems (1.61 cm^2 kg) in order to obtain reasonable failure times.

substrate by lateral crack propagation and coalescence, similar to a highly cross-linked adhesive [38]. There is no formation of foam or fibrils. Hence, the maximum elongation and, concomitantly, the debonding energy is strongly reduced. Addition of the tackifier essentially moves the adhesive in the right rheological window for foam formation. This results in substantial energy dissipation during elongation and an overall increase in debonding energy.

Finally, the influence of the amount of tackifier on the shear adhesion is examined. Figure 8 provides the data obtained for the time-to-failure (hold time) in a static shear test on the materials considered in this work. In the case of the statistical co-polymer, the hold time decreases with the quantity of tackifier and slippage is observed. As is typical for most tackified adhesives, the addition of resin to the S-co-polymer leads to a reduction of the equilibrium compliance as well as the viscosity in proportion to the resin concentration [39]. This behaviour is in stark contrast with the formulated block co-polymer, which shows a strong increase in the time-to-failure (hold time) with the amount of tackifier. The failure times are one to two orders of magnitudes higher, as compared to the statistical co-polymer. Note also that the stress exerted on the block co-polymer-based adhesives was four times higher than for the adhesives based on the statistical co-polymer. The trend observed for the shear strength of the formulated block co-polymers is quite remarkable and show that the presence of hard microdomains acting as physical cross-links substantially increases the compliance of the adhesive.

4. CONCLUSIONS

We were able to demonstrate the miscibility between a radially branched acrylic co-polymer and a rosin ester type resin up to a content of 75 phr.

In contrast to the random co-polymer, two distinct glass transitions, characteristic of a phase-separated material, were evidenced for the block co-polymer based blends. A supra-molecular ordering of spherical microdomains embedded in a continuous matrix could further be established by AFM for the block co-polymer. The Gordon–Taylor expression provides an empirical description of the dependence of T_g on tackifier content for the random co-polymer and the elastomer phase of the block co-polymer. The DSC results also suggest that the thermoplastic microdomains are partly miscible with the tackifier.

The marked difference in PSA properties between the random and block co-polymers is due to the ability of the block co-polymer to form a physical network by phase separation. Furthermore, the radial structure of the block co-polymer introduces additional chemical cross-links and, hence, produces a dense network which appreciably improves the cohesive strength of these materials. This network provides the required cohesion for suitable adhesive performance in PSAs. In contrast, the statistical co-polymer has a poor cohesive strength as a result of the low number of temporary entanglements, typical for polyacrylates.

For a sufficiently strong polymer network, the role of the tackifier is to adjust properly the adhesion/cohesion balance by controlling the rheological behavior of the system.

The results show that adhesive systems based on acrylic block co-polymers can be formulated to give tailored peel adhesion on various substrates together with high cohesive strength. Interestingly, these properties can be varied over a wide range depending on the tackifier content.

Acknowledgements

The authors wish to thank Th. Lardot for the DSC, TMA and DMA measurements and J. Vaneecke for his assistance in compounding and testing the acrylic adhesives.

REFERENCES

1. F. C. Jagisch and J. M. Tancrede, in: *Handbook of Pressure Sensitive Adhesives*, D. Satas (Ed.), pp. 346–398. Satas & Associates, Warwick, RI (1999).
2. F. S. Bates and G. H. Fredrickson, in: *Thermoplastic Elastomers*, 2nd edn, G. Holden, N. R. Legge, R. Quirck and H. E. Schroeder (Eds), pp. 335–364. Hanser, Munich (1996).
3. C. A. Dahlquist, in: *Proc. Nottingham Conf. on Adhesion*. Maclaren, London, pp. 143 (1966).
4. D. H. Kaelble, *J. Adhesion* **1**, 102 (1969).
5. D. H. Kaelble, *Trans. Soc. Rheol.* **4**, 43 (1960).
6. D. W. Bamborough and P. M. Duncley, *Adhesives Age* **33**, 20 (Nov. 1990).
7. K. W. McKay, W. A. Gros and C. F. Diehl, *J. Appl. Polym. Sci.* **56**, 947 (1995).
8. F. X. Gibert, G. Marin, C. Derail, A. Allal and J. Lechat, *J. Adhesion* **79**, 825 (2003).
9. A. Roos and C. Creton, *Macromolecules* **38**, 7807 (2005).
10. T. Matsubara, in: *Proceedings of the 27th Pressure Sensitive Tape Council TECH XXVII*, Orlando, FL, pp. 233–245 (2004).
11. J. M. Tancrede and C. F. Diehl, *Adhesives Age* **39**, 36 (Nov. 1996).

12. D. A. Dubois, in: *Proceedings of the 27th Pressure Sensitive Tape Council TECH XXVII*, Orlando, FL, pp. 185–198 (2004).
13. D. A. Shipp, J.-L. Wang and K. Matyjaszewski, *Macromolecules* **31**, 8005 (1998).
14. P. A. Mancinelli, *Adhesives Age* **32**, 18 (Sept. 1989).
15. M. Yamamoto, F. Nakano, T. Doi and Y. Moroisihi, *Int. J. Adhesion Adhesives* **22**, 37 (2002).
16. K. Hamada, Y. Morishita, T. Kurihara and K. Ishiura, in: *Proceedings of the 27th Pressure Sensitive Tape Council TECH XXVII*, Orlando, FL, pp. 53–55 (2004).
17. M. K. Mishra and S. Kobayashi, *Star and Hyperbranched Polymers*. Marcel Dekker, New York, NY (1999).
18. J. S. Shim and J. P. Kennedy, *J.Polym. Sci., Part A: Polym. Chem.* **37**, 815 (1999).
19. J. E. Puskas, P. Antony, Y. Kwon, C. Paulo, M. Kovar, P. R. Norton, G. Kaszas and V. Altstädt, *Macromol. Mater. Eng.* **286**, 565 (2001).
20. M. Jeusette, P. Leclère, R. Lazzaroni, F. Simal, J. Vaneecke, T. Lardot and P. Roose, *Macromolecules* **40**, 1055 (2007).
21. C. Creton and P. Fabre, in: *Adhesion Science and Engineering, The Mechanics of Adhesion*, D. A. Dillard and A. V. Pocius (Eds), Vol. 1, pp. 535–576. Elsevier, Amsterdam (2002).
22. F. X. Gibert, A. Allal, A. G. Marin and C. Derail, *J. Adhesion Sci. Technol.* **13**, 1029 (1999).
23. L. Benyahia, C. Verdier and J.-M. Piau, *J. Adhesion* **62**, 45 (1997).
24. C. Verdier, J.-M. Piau and L. Benyahia, *J. Adhesion* **68**, 93 (1998).
25. H.-J. Kim and H. Mizumachi, *J. Appl. Polym. Sci.* **57**, 175 (1995).
26. H.-J. Kim and H. Mizumachi, *J. Appl. Polym. Sci.* **57**, 201 (1995).
27. H.-J. Kim and H. Mizumachi, *J. Appl. Polym. Sci*. **57**, 1891 (1995).
28. Ph. Leclère, R. Lazzaroni, J.-L. Brédas, J. M. Yu, Ph. Dubois and R. Jérôme, *Langmuir* **12**, 4317 (1996).
29. J. D. Tong, Ph. Leclère, A. Rasmont, J.-L. Brédas, R. Lazzaroni and R. Jérôme, *Macromol. Chem. Phys.* **201**, 1250 (2000).
30. A. Rasmont, Ph. Leclère, C. Doneux, G. Lambin, J. D. Tong, R. Jérôme, J.-L. Brédas and R. Lazzaroni, *Colloids Surfaces B* **19**, 381 (2000).
31. J. D. Tong, Ph. Leclère, C. Doneux, J.-L. Brédas, R. Lazzaroni and R. Jérôme, *Polymer* **42**, 3503 (2001).
32. Y. Takashima and T. Hata, *J. Adhesion Soc. Jpn.* **20**, 143 (1984).
33. A. N. Gent and J. Schultz, *J. Adhesion* **3**, 281 (1972).
34. D. H. Kaelble, *Physical Chemistry of Adhesion*. Wiley, New York, NY (1971).
35. A. N. Gent and S. Y. Kaang, *J. Adhesion* **24**, 173 (1987).
36. H. W. H. Yang, *J. Appl. Polym. Sci.* **55**, 645 (1995).
37. S. G. Chu, in: *Handbook of Pressure Sensitive Adhesive Technology*, 2nd edn, D. Satas (Ed.), pp. 158–203. Van Nostrand-Reinhold, New York, NY (1989).
38. F. Deplace, C. Creton, P. Roose, F. Simal and S. van Es, in: *Proceedings of the 13th Journées d'étude sur l'Adhésion (JADH) 2005*, Bollwiller, France (2005).
39. T. G. Wood, *Adhesives Age* **30**, 19 (July 1987).